Int. J. Electrochem. Sci., 17 **(2022)** Article Number: 221041, doi: 10.20964/2022.10.39

International Journal of
ELECTROCHEMICAL
SCIENCE
www.electrochemsci.org

Short Communication

Electrochemical sensor based on antibody modified of MnO_2@CNTs/GCE for cardiac myoglobin detection in human blood serum as a sensitive marker of muscle damage

Xiao Li[1,*], *Omid Rouhi* [2,*]

[1] Anyang Vocational and Technical College, Department of public education , Henan Anyang China
[2] Department of Chemistry, Qaemshahr Branch, Islamic Azad University, Qaemshahr, Iran
[*]E-mail: lixiao3695388@sina.com, omidrouhi62@gmail.com

Received: 3 July 2022 / *Accepted:* 8 August 2022 / *Published:* 10 September 2022

The goal of the current study is to develop a sensitive and selective myoglobin (MB) electrochemical sensor as a sensitive marker of muscle damage by synthesizing a nanocomposite of MnO_2 nanostructures and carbon nanotubes (MnO_2@CNTs) by an electrodeposition method on a glassy carbon electrode surface and immobilizing myoglobin antibody (MB-Ab) on the nanocomposite surface. According to structural investigations by SEM and XRD, the MnO_2 nanostructures were anchored with edge CNTs, which provided an abundance of interstitial space in the composite. MB-Ab/MnO_2@CNTs/GCE demonstrated excellent stability, high specificity, high sensitivity (0.88994 µA/µg mL^{-1}), broad linear range (0 to 15 µg/mL), and adequate detection limit (3 ng/mL) toward recently reported MB sensors, according to electrochemical studies by DPV measurements. The usefulness and precision of the MB-Ab/MnO_2@CNTs/GCE were assessed for the detection of MB in prepared real samples of human blood serum provided by healthy volunteers. The analytical results showed acceptable recovery (96.00 % to 97.25 %) and low values of RSD (3.28 % to 4.35 %), as well as good agreement between the results of electrochemical studies and Cardiac Markers ELISA kits, proving that the MB-Ab/MnO_2 can be successfully employed to determine MB in biological samples.

Keywords: Electrodeposition; Nanocomposite; MnO_2 nanostructures; Carbon nanotubes; Myoglobin; Human blood serum; Differential pulse voltammetry

1. INTRODUCTION

A monomeric oxygen-binding protein called myoglobin (MB) has a heme prosthetic group in it [1, 2]. The heart and skeletal muscles contain the protein MB [3-5]. The MB function is similar to hibernation in that it protects the heart against brief periods of hypoxia [6, 7]. The muscles consume the oxygen that is available during exercise [8, 9]. The oxygen that is connected to MB gives the muscles extra oxygen so they can work at a high level for a longer period of time. Muscle cells contain

MB that is released into the bloodstream when the muscle is injured. Myoglobin is helped out of the circulation and into the urine by the kidneys [10-12]. The kidneys can become damaged by too much MB. MB is also released into the bloodstream during a cardiac attack. 2 to 3 hours after the onset of the first signs of muscle injury, the blood level of MB n rises [13-15]. Therefore, measuring MB offers a preliminary indicator of myocardial injury, such as that seen in myocardial infarction or reinfarction [16-18].

Therefore, the clinical applications of the diagnostic sensitivity of MB can be very useful, and many studies have been done to determine the level of MB in blood serum using ELISA [19, 20], spectrophotometric method [21, 22], fluorescence detector [23], surface plasmon resonance sensor [24], electrochemiluminescence [25, 26], colorimetric biosensor [27, 28], radioimmunoassay [29], and electrochemical sensors [30-35]. The electrochemical sensors are a precise, environmentally benign, and easy-to-use technique for the sensitive and selective measurement of MB in biological samples that contain various proteins, enzymes, and interfering inorganic and organic chemicals [36, 37]. On the other hand, using electrodes modified with nanostructures can improve the sensitivity, selectivity, and stability of electrochemical sensors [38-40].

Due to the presence of nanopores and their large specific surface area, the nanostructures graphene and CNTs are particularly useful for altering electrode surfaces and enhancing electrocatalytic current [41, 42]. Additionally, the functional groups or charged sites act as efficient active sites for assembling and anchoring metal precursors and metal oxide nanoparticles, thereby promoting their utilization and electrocatalytic activity [43-45]. Additionally, the highly electrically conductive nanoporous network of CNTs makes it easier for reagent molecules to reach the catalytic sites and enhances charge transfer in electrocatalytic reactions [46, 47]. The current study focuses on the synthesis of MnO_2@CNT nanocomposite using the electrodeposition method on the GCE surface, as well as the immobilization of MB-Ab on the nanocomposite surface.

2. EXPERIMENT

2.1. Preparation MB-Ab/MnO_2@CNTs nanostructures modified GCE

MnO_2/CNTs composite modified GCE was prepared through the electrodeposition method [48]. Briefly, 100 mg of high purity CNTs (99%, Guangzhou Hongwu Material Technology Co., Ltd., China) and 1.5 g of $KMnO_4$ (≥99%, Sigma-Aldrich) was added 1.5 g of $Mn(OAc)_2$•$4H_2O$ (≥99%, Sigma-Aldrich), and the mixture was dispersed 100 mL of deionized water under magnetic stirring for 60 minutes. Then, 0.25 mL of H_2SO_4 (97%) was added to the obtained suspension. After 30 minutes of magnetic stirring, the suspension was used as an electrodeposition electrolyte. Prior to the electrodeposition, the GCE (3 mm in diameter) surface was polished with 0.3 and 0.05 μm γ-Al_2O_3 slurry (99.99%, Sigma-Aldrich) successively and then ultrasonically washed with ethanol for 10 minutes, and followed by rinsing with deionized water. The electrodeposition of MnO_2/CNTs composite was conducted on an electrochemical workstation potentiostat (CS150, Xian Yima Optoelec Co., Ltd., China) in a three-electrode electrochemical cell setup which contained clean GCE, an

Ag/AgCl (3 M KCl) and platinum mesh as working, reference and counter electrode, respectively at a potential window from -0.05 V to 1.3 V for 50 cycles at a scan rate of 15 mV/s. The electrodeposition of pure CNTs on GCE was carried out in an electrolyte free of $KMnO_4$ and $Mn(OAc)_2•4H_2O$, while the electrodeposition of pure MnO_2 on GCE was carried out in an electrolyte free of CNTs. To prepare myoglobin antibody (MB-Ab, Sigma-Aldrich) modified electrodes, 5 mg of MB was dissolved in 10 mL of deionized water. The 100 μL of MB solution was dropped on the electrode surface followed by air drying for 10 hours. Then, the electrode was washed with deionized water three times before being used.

2.2. Instruments

To ascertain the structural characteristics of the electrodeposited sample, measurements using an X-ray diffractometer (Bruker D8 advanced X-ray diffractometer) were made. For morphological analyses, scanning electron microscopy (SEM; Hitachi S-3000H, Japan) was employed. In a workstation potentiostat galvanostat system equipped with a three-electrode electrochemical cell where bare and nanostructure modified GCE are employed as working electrodes, electrochemical experiments have been carried out using cyclic voltammetry (CV) and differential pulse voltammetry (DPV) techniques. 0.1M phosphate buffer solution (PBS) electrolyte (pH 7.4) was used for the DPV measurements. It had a 0.1M NaH2PO4 (99%, Sigma-Aldrich) and 0.1M Na2HPO4 (99%) volume ratio.

2.3. Preparation the actual sample from human blood serum

For the purpose of MB determination in prepared genuine samples of human blood serum provided by healthy volunteers, the applicability of MB-Ab/MnO_2@CNTs/GCE was assessed. The serum sample was centrifuged at 1000 rpm for 15 minutes; the supernatant that was produced was then filtered using filter paper (20 μm, Whatman), and it was used to prepare 0.1 M PBS (pH 7.0). The MB level in the ready actual sample was then determined using measurements from the DPV and Cardiac Markers ELISA kits. Using the usual addition approach, the recovery and relative standard deviation (RSD) values were obtained.

3. RESULTS AND DISCUSSION

3.1. Structural analyses

Figure 1 shows SEM images of modified GCE made with MnO_2 and MnO_2@CNT nanostructures. MnO_2 SEM micrographs Figure 1a shows how MnO_2, which is composed of several self-assembled irregular nanosheets, forms a flower-like structure on GCE. As can be seen, there are tiny porous nanoneedles with an average particle size of 80 nm. The MnO_2@CNTs nanocomposite modified GCE can be seen in Figure 1b to exhibit MnO_2 nanostructures anchored with edge CNTs that

provided a lot of interstitial space in the composite [49-51]. It can increase the effective liquid–solid interfacial area and offer enough electrochemically active sites on the surface of a nanocomposite to aid the Faraday reaction by providing a channel for the insertion and extraction of electrolyte ions [52-55].

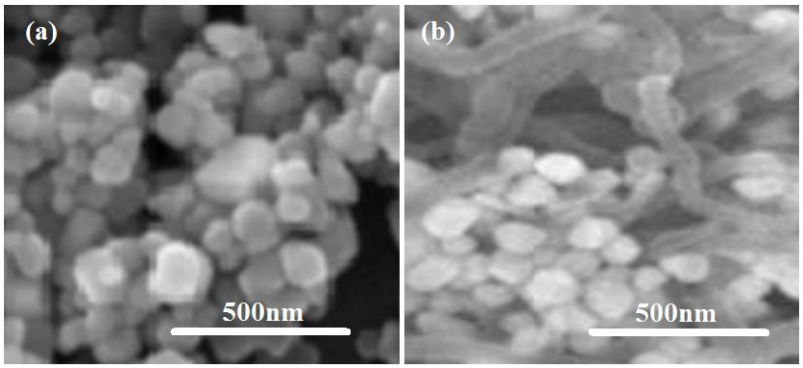

Figure 1. SEM micrographs of (a) MnO_2, (b) MnO_2@CNTs nanostructures modified GCE.

Figure 2 shows the results of the structural characterization of powders of electrodeposited CNTs, MnO_2 and MnO_2@CNTs nanostructures. The XRD profile of CNTs shows a characteristic sharp diffraction peak at 26.12° which is assigned to (002) plane of hexagonal phase graphite structured CNTs (JCPDS card No. 75–1621) [56-58]. It is observed from the XRD profile of MnO_2, there are diffraction peaks at 12.15°, 24.71°, 35.58° and 65.96° which are indexed to (001), (002), (111), and (312) crystalline planes of the birnessite-type crystal structure of MnO_2, respectively (JCPDS card No. 42- 1317) [52, 59, 60]. The XRD profile of MnO_2@CNTs nanocomposite depicts characteristic diffraction peak (002) of CNTs and (001), (002), (111), and (312) crystalline planes MnO_2, demonstrating the successful electrodeposition of well-crystalline MnO_2@CNTs nanocomposite on GCE [61-63].

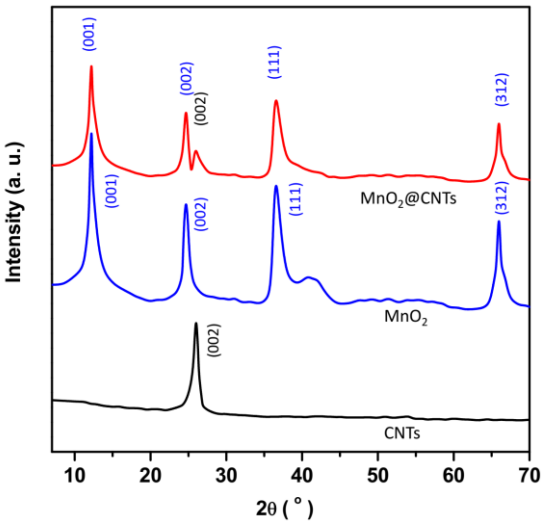

Figure 2. Results of structural characterization of powders of electrodeposited CNTs, MnO_2 and MnO_2@CNTs nanostructures.

3.2. Electrochemical analyses

Figure 3 shows the DPV curves of the following materials: bare GCE, CNTs/GCE, MnO_2/GCE, MnO_2@CNTs/GCE, MB-Ab/CNTs/GCE, MB-Ab/MnO_2/GCE, and MB-Ab/MnO_2@CNTs/GCE in the potential window of 0.0V to 0.6 V with a scanning rate of 50 mV/s in 0.1 M PBS (pH 7.0). The DPV curves of bare GCE, CNTs/GCE, MnO_2/GCE, and MnO_2@CNTs/GCE do not show any peaks, but the curves of MB-Ab/CNTs/GCE, MB-Ab/MnO_2/GCE, and MB-Ab/MnO_2@CNTs/GCE exhibit anodic peaks at 0.31 V, 0.33 V and 0.30 V, respectively, due to the immobilization of MB-Ab on the surface.of electrodes. Myoglobin contains a porphyrin ring with an iron at its center [26], and these peaks are asociated with the reduction of electroactive MB where MB-Fe(III) gets reduced to MB-Fe (II) [64].

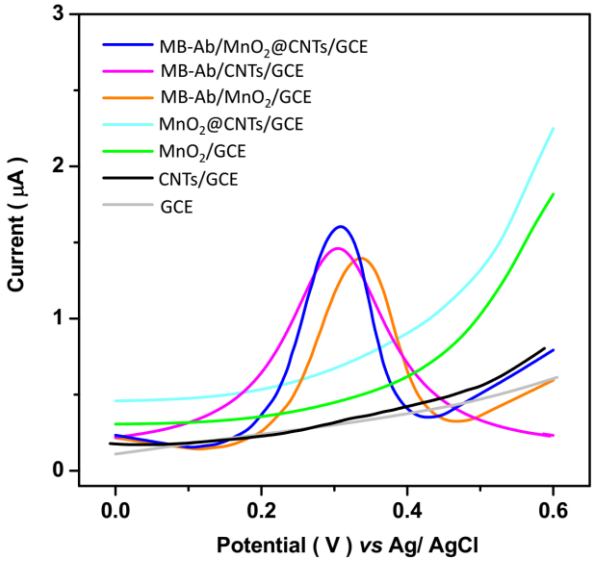

Figure 3. The DPV curves of bare GCE, CNTs/GCE, MnO_2/GCE, MnO_2@CNTs/GCE, MB-Ab/CNTs/GCE, MB-Ab/MnO_2/GCE, MB-Ab/MnO_2@CNTs/GCE at the potential window from 0.0V to 0.6 V with a scanning rate of 50 mV/s in 0.1 M PBS (pH 7.0).

Further electrochemical investigation was carried out for the analysis of the stability of the electrochemical response of MB-Ab/CNTs/GCE, MB-Ab/MnO_2/GCE, and MB-Ab/MnO_2@CNTs/GCE. Figure 4 exhibits the resultant first and 120th CV curves of all electrodes at the potential window from 0.0 V to 0.6 V with a scanning rate of 50 mV/s in 0.1 M PBS (pH 7.0) [65-67]. As seen, the first CV curve and subsequent CV response after 120 scans show a 6%, 11%, and 4% decrease in the current peak of MB-Ab/CNTs/GCE, MB-Ab/MnO_2/GCE, and MB-Ab/MnO_2/GCE, respectively. It is illustrated that the high stability of electrochemical response of MB-

Ab/MnO_2@CNTs/GCE is due to the successful immobilization of MB-Ab molecules on MnO_2@CNTs nanocomposite which resulted in good biocompatibility for maintenance of the biological activity of Mb [64, 68]. Thus, the following electrochemical analyses were conducted on MB-Ab/MnO_2@CNTs/GCE [69, 70].

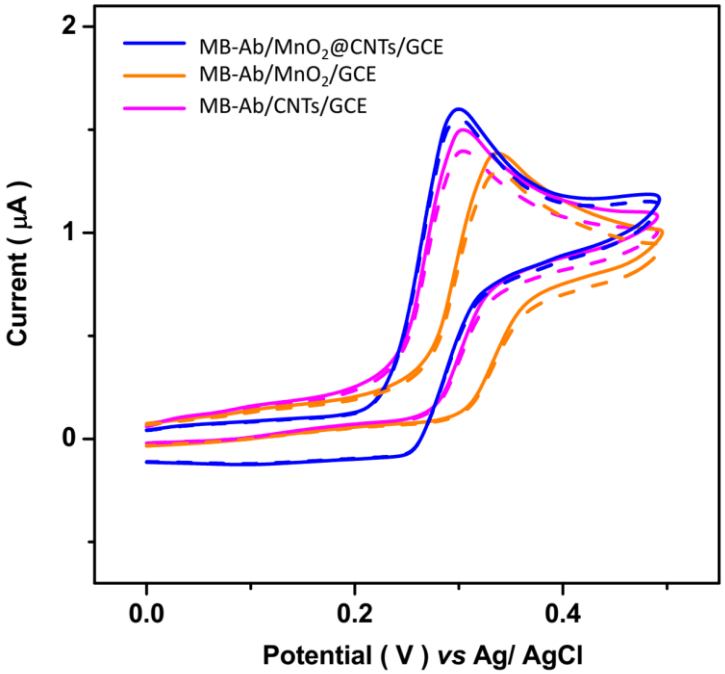

Figure 4. The resulted first (solid line) and 120th (dashed line) CV curves of MB-Ab/CNTs/GCE, MB-Ab/MnO_2/GCE, MB-Ab/MnO_2@CNTs/GCE at the potential window from 0.0V to 0.6 V with a scanning rate of 5 mV/s in 0.1 M PBS (pH 7.0).

Figure 5 shows the DPV behavior of MB-Ab/MnO_2@CNTs/GCE in response to repeated injections of 1 g/mL MB solution in 0.1 M PBS (pH 7.0) in the potential window of 0.0 V to 0.6 V with a scanning rate of 50 mV/s. It is revealed that the DPV response exhibits an increase in peak current intensity after the addition of each 1 g/mL MB electrochemical cell. The calibration plot shown in Figure 5 shows that the peak current intensities of the DPV responses grow linearly over the concentration range of 0 to 15µg/mL, and the MB-Ab/MnO2@CNTs/GCE is determined to have a sensitivity of 0.88994 µA/µg mL^{-1}. The results indicate that a detection limit of 3 ng/mL (S/N = 3) can be estimated [71-73]. A comparison between analytical figures of merit of MB-Ab/MnO_2@CNTs/GCE and some reported MB sensors is tabulated in Table 1. The developed method in the presence study shows the linear range and detection limit of MB-Ab/MnO_2@CNTs/GCE are promoted and acceptable because the MnO_2@CNTs nanocomposite provides good electrical properties and simple chemical functionality for the development of compatible bio-interface on the electrode surface, as well as the presence of high quality specific antibodies/aptamers for recognition/capture of MB molecules [74-76]. Moreover, MnO_2@CNTs nanocomposite delivers the highest edge density, large surface area and high stability which significantly improved the electrocatalytic ability and stability of immobilized MB molecules for direct electrochemistry and direct electron transfer [77-80].

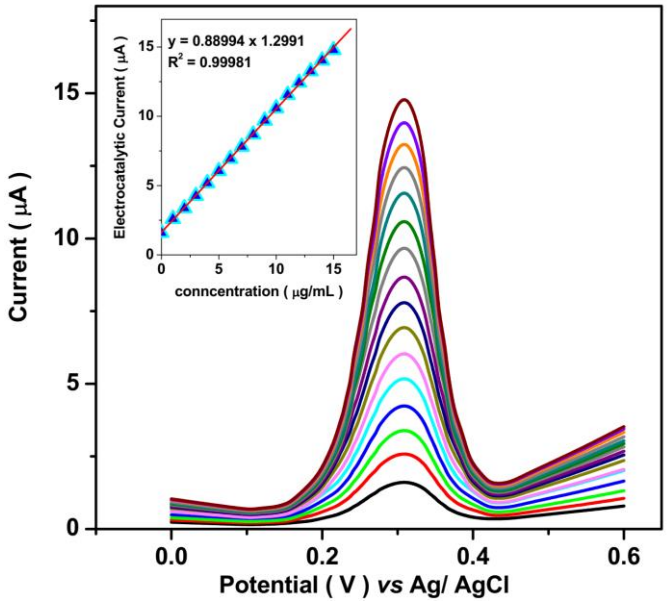

Figure 5. The DPV response of MB-Ab/MnO_2@CNTs/GCE to consecutive injections of 1 µg/mL MB solution in 0.1 M PBS (pH 7.0) at the potential window from 0.0 V to 0.6 V with a scanning rate of 50 mV/s.

Table 1. Comparison between analytical figures of merit of MB-Ab/MnO_2@CNTs/GCE and some reported MB sensors.

Electrodes	Technique	Detection limit (ng/ml)	Linear range (µg/ml)	Ref.
MB-Ab/MnO_2@CNTs/GCE	DPV	3	0 to 15	This work
MB-Ab/didodecyldimethylammonium bromide /Au NPs	CV	10	0.01 to 1.780	[30]
MB-Ab/didodecyldimethylammonium bromide /Au NPs	SV	4.4	0.0178 to 1.780	[33]
Molecularly imprinted polymer /Au/screen printed electrode	SWV	2250	1.1 to 2.98	[31]
Smart plastic antibody material /Au/screen printed electrode	SWV	280	3.5 to 0.58	[32]
MB-Ab/graphene quantum dots/screen printed electrode	DPV	0.01	0.00001 to 0.1	[35]
MB/rGO/CNTs	CV	0.34	0.001 to 4	[34]

SWV: Square wave voltammetry; SV: Stripping voltammetry

The ability of MB-Ab/MnO_2@CNTs/GCE to identify MB in the presence of certain chemicals found in biological liquids was assessed. Table 2 provides an overview of the electrocatalytic signal of DPV measurement in 0.1 M PBS (pH 7.0) at the potential window of 0.0 V to 0.6 V with a scanning

rate of 50 mV/s to successive injections of 1 g/mL MB solution and 10 g/mL of substances. The electrocatalytic signal of MB-Ab/MnO_2@CNTs/GCE is found to be quite strong upon the addition of MB solution, and there is no discernible change in the electrocatalytic signal of MB upon the addition of interfering chemicals in the electrolyte solution [76, 81, 82]. One might infer that the MB-Ab/MnO_2@CNTs/GCE can be thought of as a particular MB sensor [83, 84]. The polymer scaffold of the MIP MIPs as a recognition element provides specificity by substrate binding to the cavities and target analytes to generate an electrochemical signal [85, 86]. The synergistic effect of the biomolecular recognition units and nanostructured MnO_2@CNTs nanocomposite forms an enhanced sensing platform with sensitivity and selectivity for MB [74, 87].

Table 2. The results of electrocatalytic signal of DPV measurement in 0.1 M PBS (pH 7.0) at peak potential of 0.6 V with a scanning rate of 50 mV/s to consecutive injections of 1 µg/mL MB solution and 10 µg/mLof substances.

Substance	**Added (µg/mL)**	**Electrocatalytic signal (µA)**	**RSD**
MB	1	0.8901	±0.0122
l-Cystine	10	0.0212	±0.0027
L-histidine	10	0.0344	±0.0021
Hemoglobin	10	0.0311	±0.0012
Bovine serum albumin	10	0.0443	±0.0011
Glucose	10	0.0250	±0.0010
Cytochrome C	10	0.0211	±0.0010
Ascorbic acid	10	0.0312	±0.0012
Glycine	10	0.0321	±0.0013
Troponin I	10	0.0244	±0.0015
Avidin	10	0.0162	±0.0017
Creatine kinase	10	0.0352	±0.0016
K^+	10	0.0247	±0.0014
Mg^{2+}	10	0.0395	±0.0013
NO_3^-	10	0.0114	±0.0012

For the purpose of determining MB, the applicability and precision of MB-Ab/MnO_2@CNTs/GCE were assessed using prepared genuine samples of human blood serum donated by healthy volunteers. Table 3 shows the outcomes of a DPV measurement in 0.1 M PBS (pH 7.0) at the potential window of 0.0 V to 0.6 V with a scanning rate of 50 mV/s before and after the addition of MB, as well as the results of analytical calculations made using the conventional addition method. The results of electrochemical studies and Cardiac Markers ELISA kits for MB determination showed acceptable recovery (96.00 percent to 97.25 percent), low values of RSD (3.28 percent to 4.35 percent), and good agreement between the results of both analyses, proving that the MB-Ab/MnO_2@CNTs/GCE can be used to successfully determine MB in biological samples.

Table 2. The findings of electrochemical studies *and* Cardiac Markers ELISA kit *for determination* MB in prepared real samples of human blood serum.

	DPV measurement			*Cardiac Markers ELISA kit*		
Spiked (µg/mL)	**detected (µg/mL)**	**Recovery (%)**	**RSD (%)**	**detected (µg/mL)**	**Recovery (%)**	**RSD (%)**
0.00	0.00	---	4.13	0.00	---	3.65
1.00	0.96	96.00	4.35	0.97	97.00	4.15
2.00	1.93	96.50	3.28	1.98	99.00	3.96
4.00	3.89	97.25	3.77	3.95	98.75	4.07

4. CONCLUSION

This research focused on creating a sensitive and specific MB electrochemical sensor using MB-Ab/MnO_2@CNTs/GCE. The MnO_2@CNT nanocomposite was created using the electrodeposition method on a GCE surface, and MB-Ab molecules were immobilized on the surface of the nanocomposite. The successful electrodeposition of a well-crystalline MnO_2@CNTs nanocomposite on GCE was indicated by structural analysis. The MB-Ab/MnO_2@CNTs/GCE demonstrated excellent stability, high specificity, high sensitivity (0.88994 µA/µg mL^{-1}), broad linear range (0 to 15 µg/mL), and adequate detection limit (3 ng/mL) toward recently reported MB sensors, according to DPV measurements. In order to determine MB in prepared real samples of human blood serum provided by healthy volunteers, the applicability and accuracy of MB-Ab/MnO_2@CNTs/GCE were assessed. The analytical results obtained indicated acceptable recovery and low values of RSD as well as good agreement between the results of electrochemical studies and Cardiac Markers ELISA kits, proving that the MB-Ab/MnO_2@CNTs/GCE can be successfully employed to determine MB in biological samples.

References

1. M.H. Mannino, R.S. Patel, A.M. Eccardt, B.E. Janowiak, D.C. Wood, F. He and J.S. Fisher, *Antioxidants*, 9 (2020) 549.
2. Z. Zhuo, Y. Wan, D. Guan, S. Ni, L. Wang, Z. Zhang, J. Liu, C. Liang, Y. Yu and A. Lu, *Advanced Science*, 7 (2020) 1903451.
3. H. Qi, Z. Hu, Z. Yang, J. Zhang, J.J. Wu, C. Cheng, C. Wang and L. Zheng, *Analytical chemistry*, 94 (2022) 2812.
4. H. Maleh, M. Alizadeh, F. Karimi, M. Baghayeri, L. Fu, J. Rouhi, C. Karaman, O. Karaman and R. Boukherroub, *Chemosphere*, (2021) 132928.
5. M. Akbari and R. Elmi, *Case reports in medicine*, 2017 (2017) 1.
6. H. Kitagishi and K. Kano, *Chemical Communications*, 57 (2021) 148.
7. S. Sun, H. Liu, Y. Hu, Y. Wang, M. Zhao, Y. Yuan, Y. Han, Y. Jing, J. Cui and X. Ren, *Bioactive Materials*, 20 (2023) 166.

8. L. Tang, Y. Zhang, C. Li, Z. Zhou, X. Nie, Y. Chen, H. Cao, B. Liu, N. Zhang and Z. Said, *Chinese Journal of Mechanical Engineering*, 35 (2022) 1.
9. N. Naderi, M. Hashim and J. Rouhi, *International Journal of Electrochemical Science*, 7 (2012) 8481.
10. B.K. Patel, N. Sepay and A. Mahapatra, *New Journal of Chemistry*, 44 (2020) 19555.
11. X. Xue, H. Liu, S. Wang, Y. Hu, B. Huang, M. Li, J. Gao, X. Wang and J. Su, *Composites Part B: Engineering*, 237 (2022) 109855.
12. M. Khosravi, *Journal of Eating Disorders*, 8 (2020) 1.
13. J.-P. Mahy, F. Avenier, W. Ghattas, R. Ricoux and M. Salmain, *Enzymes for Solving Humankind's Problems*, 60 (2021) 363.
14. J. Lei, Y. Dong, Q. Hou, Y. He, Y. Lai, C. Liao, Y. Kawamura, J. Li and B. Zhang, *Frontiers in nutrition*, 9 (2022) 747705.
15. X. Wang, C. Li, Y. Zhang, H.M. Ali, S. Sharma, R. Li, M. Yang, Z. Said and X. Liu, *Tribology International*, 174 (2022) 107766.
16. H. Zhu, M. Zhang, P. Wang, C. Sun, W. Xu, J. Ma, Y. Zhu and D. Wang, *Food Chemistry*, 382 (2022) 132354.
17. Q. Zou, P. Xing, L. Wei and B. Liu, *Rna*, 25 (2019) 205.
18. H. Karimi-Maleh, R. Darabi, M. Shabani-Nooshabadi, M. Baghayeri, F. Karimi, J. Rouhi, M. Alizadeh, O. Karaman, Y. Vasseghian and C. Karaman, *Food and Chemical Toxicology*, 162 (2022) 112907.
19. T. Kitao, S. Miyaishi and H. Ishizu, *Forensic science international*, 71 (1995) 205.
20. Q. Hou, J. Huang, X. Xiong, Y. Guo and B. Zhang, *Journal of Crohn's and Colitis*, 20 (2022) 1.
21. I. Hassinen, J. Hiltunen and T. Takala, *Cardiovascular Research*, 15 (1981) 86.
22. J. Rouhi, M. Alimanesh, R. Dalvand, C.R. Ooi, S. Mahmud and M.R. Mahmood, *Ceramics International*, 40 (2014) 11193.
23. F. Darain, P. Yager, K.L. Gan and S.C. Tjin, *Biosensors and Bioelectronics*, 24 (2009) 1744.
24. B. Osman, L. Uzun, N. Beşirli and A. Denizli, *Materials Science and Engineering: C*, 33 (2013) 3609.
25. M.R.K. Pur, M. Hosseini, F. Faridbod and M.R. Ganjali, *Microchimica Acta*, 184 (2017) 3529.
26. Y. Zhang, H.N. Li, C. Li, C. Huang, H.M. Ali, X. Xu, C. Mao, W. Ding, X. Cui and M. Yang, *Friction*, 10 (2022) 803.
27. Q. Wang, X. Yang, X. Yang, F. Liu and K. Wang, *Sensors and Actuators B: Chemical*, 212 (2015) 440.
28. M. Akbari, R. Moghadam, R. Elmi, A. Nosrati, E. Taghiabadi and N. Aghdami, *Journal of Ophthalmic and Vision Research*, 14 (2019) 400.
29. G. Gilkeson, M.J. Stone, M. Waterman, R. Ting, C.E. Gomez-Sanchez, A. Hull and J.T. Willerson, *American Heart Journal*, 95 (1978) 70.
30. E. Suprun, T. Bulko, A. Lisitsa, O. Gnedenko, A. Ivanov, V. Shumyantseva and A. Archakov, *Biosensors and Bioelectronics*, 25 (2010) 1694.
31. F.T.C. Moreira, R.A.F. Dutra, J.P.C. Noronha and M.G.F. Sales, *Electrochimica Acta*, 107 (2013) 481.
32. F.T.C. Moreira, S. Sharma, R.A.F. Dutra, J.P.C. Noronha, A.E.G. Cass and M.G.F. Sales, *Biosensors and Bioelectronics*, 45 (2013) 237.
33. V.V. Shumyantseva, T.V. Bulko, M.Y. Vagin, E.V. Suprun and A.I. Archakov, *Biochemistry (Moscow) Supplement Series B: Biomedical Chemistry*, 4 (2010) 237.
34. V. Kumar, M. Shorie, A.K. Ganguli and P. Sabherwal, *Biosensors and Bioelectronics*, 72 (2015) 56.
35. S.K. Tuteja, R. Chen, M. Kukkar, C.K. Song, R. Mutreja, S. Singh, A.K. Paul, H. Lee, K.-H. Kim, A. Deep and C.R. Suri, *Biosensors and Bioelectronics*, 86 (2016) 548.

36. M. Liu, C. Li, Y. Zhang, Q. An, M. Yang, T. Gao, C. Mao, B. Liu, H. Cao and X. Xu, *Frontiers of Mechanical Engineering*, 16 (2021) 649.
37. Y. Yang, M. Yang, C. Li, R. Li, Z. Said, H. Muhammad Ali and S. Sharma, *Frontiers of Mechanical Engineering*, (2022) 1.
38. T. Li, D. Shang, S. Gao, B. Wang, H. Kong, G. Yang, W. Shu, P. Xu and G. Wei, *Biosensors*, 12 (2022) 314.
39. X. Wu, C. Li, Z. Zhou, X. Nie, Y. Chen, Y. Zhang, H. Cao, B. Liu, N. Zhang and Z. Said, *The International Journal of Advanced Manufacturing Technology*, 117 (2021) 2565.
40. M. Khosravi, *Open Access Macedonian Journal of Medical Sciences*, 8 (2020) 553.
41. W. Liu, Y. Zheng, Z. Wang, Z. Wang, J. Yang, M. Chen, M. Qi, S. Ur Rehman, P.P. Shum and L. Zhu, *Advanced Materials Interfaces*, 8 (2021) 2001978.
42. T. Gao, Y. Zhang, C. Li, Y. Wang, Q. An, B. Liu, Z. Said and S. Sharma, *Scientific reports*, 11 (2021) 1.
43. S.E. Baghbamidi, H. Beitollahi, S. Tajik and R. Hosseinzadeh, *International Journal of Electrochemical Science*, 11 (2016) 10874.
44. S. Themsirimongko, N. Promsawan and S. Saipanya, *International Journal of Electrochemical Science*, 11 (2016) 967.
45. H. Karimi-Maleh, C. Karaman, O. Karaman, F. Karimi, Y. Vasseghian, L. Fu, M. Baghayeri, J. Rouhi, P. Senthil Kumar and P.-L. Show, *Journal of Nanostructure in Chemistry*, (2022) 1.
46. T.-W. Chen, X.-N. Yu and S.-J. Li, *International Journal of Electrochemical Science*, 14 (2019) 7037.
47. J. Liu, T. Li, H. Zhang, W. Zhao, L. Qu, S. Chen and S. Wu, *Materials Today Bio*, 14 (2022) 100243.
48. A. Zakaria and D. Leszczynska, *Chemosensors*, 7 (2019) 1.
49. T. Li, W. Yin, S. Gao, Y. Sun, P. Xu, S. Wu, H. Kong, G. Yang and G. Wei, *Nanomaterials*, 12 (2022)
50. M. Yang, C. Li, Z. Said, Y. Zhang, R. Li, S. Debnath, H.M. Ali, T. Gao and Y. Long, *Journal of Manufacturing Processes*, 71 (2021) 501.
51. H. Karimi-Maleh, H. Beitollahi, P.S. Kumar, S. Tajik, P.M. Jahani, F. Karimi, C. Karaman, Y. Vasseghian, M. Baghayeri and J. Rouhi, *Food and Chemical Toxicology*, (2022) 112961.
52. L. Li, Z.A. Hu, N. An, Y.Y. Yang, Z.M. Li and H.Y. Wu, *The Journal of Physical Chemistry C*, 118 (2014) 22865.
53. J. Yan, Y. Yao, S. Yan, R. Gao, W. Lu and W. He, *Nano Letters*, 20 (2020) 5844.
54. X. Cui, C. Li, Y. Zhang, W. Ding, Q. An, B. Liu, H.N. Li, Z. Said, S. Sharma, R. Li and S. Debnath, *Frontiers of Mechanical Engineering*, (2022) 1.
55. M. Khosravi, *European journal of translational myology*, 31 (2021) 9411.
56. X. Qi, Q. Hu, H. Cai, R. Xie, Z. Bai, Y. Jiang, S. Qin, W. Zhong and Y. Du, *Scientific reports*, 6 (2016) 1.
57. T. Li, M. Sun and S. Wu, *Nanomaterials*, 12 (2022) 784.
58. T. Gao, C. Li, Y. Wang, X. Liu, Q. An, H.N. Li, Y. Zhang, H. Cao, B. Liu and D. Wang, *Composite Structures*, 286 (2022) 115232.
59. W. Yang, W. Liu, X. Li, J. Yan and W. He, *Journal of Advanced Research*, (2022) 1.
60. K. Abbasi, M. Hazrati, A. Mohammadbeigi, J. Ansari, M. Sajadi, A. Hosseinnazzhad and E. Moshiri, *Indian Journal of Medical and Paediatric Oncology*, 37 (2016) 227.
61. D. Shi, Y. Chen, Z. Li, S. Dong, L. Li, M. Hou, H. Liu, S. Zhao, X. Chen and C.P. Wong, *Small Methods*, (2022) 2200329.
62. Y. Yang, H. Zhu, X. Xu, L. Bao, Y. Wang, H. Lin and C. Zheng, *Microporous and Mesoporous Materials*, 324 (2021) 111289.
63. Z. Duan, C. Li, Y. Zhang, M. Yang, T. Gao, X. Cui, R. Li, Z. Said, S. Debnath and S. Sharma, *Frontiers of Mechanical Engineering*, (2022) 1.

64. A.T.E. Vilian, V. Veeramani, S.-M. Chen, R. Madhu, C.H. Kwak, Y.S. Huh and Y.-K. Han, *Scientific Reports*, 5 (2015) 18390.
65. Z. Li, M. Teng, Y. Jiang, L. Zhang, X. Luo, Y. Liao and B. Yang, *Frontiers in Immunology*, 13 (2022) 857727.
66. H. Li, Y. Zhang, C. Li, Z. Zhou, X. Nie, Y. Chen, H. Cao, B. Liu, N. Zhang and Z. Said, *The International Journal of Advanced Manufacturing Technology*, 120 (2022) 1.
67. N. Farshchian, V. Farnia, M. Reza Aghaiani and N. Abdoli, *Current drug safety*, 8 (2013) 257.
68. K. Jin, Y. Yan, M. Chen, J. Wang, X. Pan, X. Liu, M. Liu, L. Lou, Y. Wang and J. Ye, *Acta Ophthalmologica*, 100 (2022) e512.
69. M. Khosravi, *Pharmacopsychiatry*, 55 (2022) 16.
70. J. Rouhi, C.R. Ooi, S. Mahmud and M.R. Mahmood, *Electronic Materials Letters*, 11 (2015) 957.
71. B. Huang, L. Changhe, Y. Zhang, D. Wenfeng, Y. Min, Y. Yuying, Z. Han, X. Xuefeng, W. Dazhong and S. Debnath, *Chinese Journal of Aeronautics*, 34 (2021) 1.
72. A.E. Anqi, C. Li, H.A. Dhahad, K. Sharma, E.-A. ATTIA, A. Abdelrahman, A.G. Mohammed, S. Alamri and A.A. Rajhi, *Journal of Energy Storage*, 52 (2022) 104906.
73. K. Salehi, A. Kordlu and R. Rezapour-Nasrabad, *Studies on Ethno-Medicine*, 14 (2020) 24.
74. Y. Wang, M. Han, X. Ye, K. Wu, T. Wu and C. Li, *Microchimica Acta*, 184 (2017) 195.
75. Z. Li, M. Teng, R. Yang, F. Lin, Y. Fu, W. Lin, J. Zheng, X. Zhong, X. Chen and B. Yang, *Sensors and Actuators B: Chemical*, 361 (2022) 131691.
76. T. Gao, Y. Zhang, C. Li, Y. Wang, Y. Chen, Q. An, S. Zhang, H.N. Li, H. Cao and H.M. Ali, *Frontiers of Mechanical Engineering*, 17 (2022) 1.
77. V. Mani, B. Dinesh, S.-M. Chen and R. Saraswathi, *Biosensors and Bioelectronics*, 53 (2014) 420.
78. C. Liu, Y. Wang, L. Li, D. He, J. Chi, Q. Li, Y. Wu, Y. Zhao, S. Zhang and L. Wang, *Journal of Controlled Release*, 349 (2022) 679.
79. H. Li, Y. Zhang, C. Li, Z. Zhou, X. Nie, Y. Chen, H. Cao, B. Liu, N. Zhang and Z. Said, *Korean Journal of Chemical Engineering*, 39 (2022) 1107.
80. N. Farshchian, S.T. Nezhad and P.B. Kamangar, *Australasian Medical Journal (Online)*, 11 (2018) 326.
81. J. Zhang, C. Li, Y. Zhang, M. Yang, D. Jia, G. Liu, Y. Hou, R. Li, N. Zhang and Q. Wu, *Journal of Cleaner Production*, 193 (2018) 236.
82. B. Li, C. Li, Y. Zhang, Y. Wang, D. Jia and M. Yang, *Chinese Journal of Aeronautics*, 29 (2016) 1084.
83. J. Zheng, R. Yue, R. Yang, Q. Wu, Y. Wu, M. Huang, X. Chen, W. Lin, J. Huang and X. Chen, *Frontiers in Bioengineering and Biotechnology*, 10 (2022) 1051.
84. Z. Said, M. Ghodbane, B. Boumeddane, A.K. Tiwari, L.S. Sundar, C. Li, N. Aslfattahi and E. Bellos, *Solar Energy Materials and Solar Cells*, 239 (2022) 111633.
85. A. Yarman and F.W. Scheller, *Sensors*, 20 (2020) 2677.
86. B. Cui, P. Liu, X. Liu, S. Liu and Z. Zhang, *Journal of Materials Research and Technology*, 9 (2020) 12568.
87. S. Pakapongpan, R. Palangsuntikul and W. Surareungchai, *Electrochimica Acta*, 56 (2011) 6831.